

1
2
3
4
5
6
7
8
9
10
11
12
13
14
15
16
17
18
19
20
21
22
23
24
25
26
27
28

Marionette: *E. coli* containing 12 highly-optimized small molecule sensors

Adam J. Meyer¹, Thomas H. Segall-Shapiro¹, and Christopher A. Voigt^{1,*}

¹ Synthetic Biology Center, Department of Biological Engineering, Massachusetts Institute of Technology, Cambridge, MA 02139, USA

*Correspondence and request for materials should be addressed to C.A.V. (cavoigt@gmail.com)

Key words: *Synthetic biology, directed evolution, biosensor, gene expression*

29 **Cellular processes are carried out by many interacting genes and their study and optimization requires**
30 **multiple levers by which they can be independently controlled. The most common method is via a**
31 **genetically-encoded sensor that responds to a small molecule (an “inducible system”). However, these**
32 **sensors are often suboptimal, exhibiting high background expression and low dynamic range. Further,**
33 **using multiple sensors in one cell is limited by cross-talk and the taxing of cellular resources. Here, we**
34 **have developed a directed evolution strategy to simultaneously select for less background, high**
35 **dynamic range, increased sensitivity, and low crosstalk. Libraries of the regulatory protein and output**
36 **promoter are built based on random and rationally-guided mutations. This is applied to generate a set**
37 **of 12 high-performance sensors, which exhibit >100-fold induction with low background and cross-**
38 **reactivity. These are combined to build a single “sensor array” and inserted into the genomes of *E. coli***
39 **MG1655 (wild-type), DH10B (cloning), and BL21 (protein expression). These “Marionette” strains allow**
40 **for the independent control of gene expression using 2,4-diacetylphosphoglucinol (DAPG), cuminic**
41 **acid (Cuma), 3-oxohexanoyl-homoserine lactone (OC6), vanillic acid (Van), isopropyl β -D-1-**
42 **thiogalactopyranoside (IPTG), anhydrotetracycline (aTc), L-arabinose (Ara), choline chloride (Cho),**
43 **naringenin (Nar), 3,4-dihydroxybenzoic acid (DHBA), sodium salicylate (Sal), and 3-**
44 **hydroxytetradecanoyl-homoserine lactone (OHC14).**

45 Advances in biology are often tied to new methods that use external stimuli to control the levels
46 of gene expression¹⁻³. Pioneered in the early 1980s, so-called inducible systems were developed that allow
47 genes to be turned on by adding a small molecule inducer to the growth media⁴. These consist of a protein
48 transcription factor (*e.g.*, LacI) whose binding to a DNA operator in a promoter is controlled by the inducer
49 (*e.g.*, IPTG). Initially co-opted from natural regulatory networks, over the years many versions were
50 designed to improve performance. In the 1990s, additional systems were developed that responded to
51 other inducers, notably arabinose and aTc, which became common tools in the field. In 1997, Lutz and
52 Bujard published a seminal paper that combined three (IPTG, arabinose, aTc) that could be easily
53 interchanged on a two-plasmid system⁵. Its organizational simplicity, compatibility, and quantified
54 response functions were revolutionary. Beyond providing a new tool to biologists to control multiple
55 genes with independent “strings,” it facilitated researchers with quantitative backgrounds to enter
56 biology⁶⁻⁷. Armed with the new ability to control two genes with precision, physicists and engineers built
57 the first synthetic genetic circuits, performed single molecule experiments inside cells, deconstructed the
58 origins of noise in gene expression, determined how enzyme balancing impacts metabolic flux, elucidated
59 rules underlying the assembly of molecular machines, and built synthetic symbiotic microbial
60 communities, just to highlight a few⁸⁻¹⁹.

61 Sensor performance is quantified by its response function; in other words, how the concentration
62 of inducer changes the activity of the output promoter (Figure 1a). Often, this promoter retains a residual
63 activity in the absence of inducer (“leakiness”). This hampers the ability to explore low expression levels
64 or keep a gene in the off state, particularly needed for toxic proteins²⁰⁻²¹. Another important parameter is
65 the dynamic range, defined as the ratio of promoter activity in the on and off states. When this is large,
66 both high and low expression can be explored as well as many intermediate states. The sensitivity is the
67 concentration of inducer that turns a sensor on (defined as 50% activation). A lower sensitivity reduces
68 the amount of a chemical that must be added to the media. Further, when multiple sensors are combined
69 into one cell, they can interfere with each other’s response functions (Figure 1b). Some small molecules
70 bind non-cognate regulators and this can lead to off-target activation (cross reactivity) or competitive
71 inhibition with the cognate small molecule (antagonism)²²⁻²⁷. Finally, each sensor requires cellular
72 resources (*e.g.*, ribosomes) to function and the activation of one sensor can influence another indirectly
73 due to resource competition²⁸. Each sensor also requires ~1-2 kb of DNA and this becomes increasingly
74 difficult to carry on plasmids. These challenges limit the number of sensors that can be put in a single cell
75 and the maximum reported to date is four²⁹.

76 Sensors can be improved using biophysical models, rational engineering and directed evolution⁵,
77 ^{23, 26, 30-36}. Improving performance requires that screens or selections be performed in the presence and
78 absence of inducer³⁷. Such dual selections have been accomplished by sorting cells based low and high
79 fluorescence, utilizing proteins that can be both toxic and selective (*e.g.*, TetA or HSV-TK), or by deploying
80 separate positive and negative selections^{26, 35, 37-44}. This has been applied to improving the response
81 functions and eliminating cross-reactivity between pairs of regulators^{23, 26, 35, 45}.

82 Here, we have developed a selection methodology that allows us to intervene at multiple steps in
83 order to simultaneously select for improved response functions and decreased crosstalk (Figure 1c). First,
84 we built 12 sensors that respond to different small molecules and made directed changes in order to
85 improve function. These sensors were then subjected to multiple rounds of negative-positive selection.
86 Negative selection is facilitated by a promiscuous A294G mutant of the phenylalanine aminoacyl tRNA-
87 synthetase (PheS)⁴⁶. In the absence of inducer, leaky transcription of PheS leads to the charging of
88 phenylalanyl-tRNA with the non-canonical amino acid 4-Chloro-DL-phenylalanine (Cl-Phe). Adding more
89 Cl-Phe increases the stringency of the selection by making PheS transcription more toxic^{43, 47}. Positive
90 selection is facilitated by a thermostable DNA polymerase (DNAP), either KOD DNAP from the archaea
91 *Thermococcus kodakarensis*⁴⁸ (for stringent replication) or the engineered PK6 DNAP⁴⁹ (to introduce
92 mutations). In the presence of inducer, the level of DNAP can be quantified by PCR amplification of the

93 sensor library after the cells are emulsified with primers⁵⁰⁻⁵¹. Multiple properties of the response function
94 can be simultaneously improved during one cycle of negative-positive selection and stringency altered by
95 changing the concentrations of Cl-Phe and inducer. Further, cross reactions can be selected against by
96 adding the inducer or regulator from a problematic system. The dual selection is applied over multiple
97 rounds to create a highly-optimized set of sensors. From these, we identify 12 that can be used together
98 in a single strain, and these are combined and integrated into the genomes of *E. coli* MG1655, DH10B, and
99 BL21 in order to create the Marionette family of strains. Genome integration increases stability and
100 reduces the cellular resources required to maintain regulator expression. It also simplifies the use of the
101 inducible systems, where only the output promoters need to be incorporated into a design (*e.g.*, for the
102 expression of multiple proteins from a plasmid).

103 An initial set of 17 putative sensors were designed. Each sensor consists of a weak constitutive
104 promoter (P_{LacI} , Supplementary Table 1) driving the expression of the regulatory gene and an output
105 promoter that is acted on by the regulator. The regulatory genes were either codon optimized and
106 synthesized or cloned (Methods and Supplementary Table 4). The output promoters were either
107 obtained from the literature or, in the case of P_{Van} , rationally designed by inserting cognate operator
108 sequences into unregulated promoters (Supplementary Table 1). The activity of the output promoter was
109 measured through the expression of yellow fluorescent protein (YFP) using flow cytometry and reported
110 in relative promoter units (RPU) (Supplementary Figure 1 and Methods). Each complete sensor was
111 cloned into the same sensor plasmid architecture (Supplementary Figure 2). Some sensors require
112 additional genes, which are encoded as an operon with the regulatory protein. For the Ara-inducible
113 system, the transporter *araE* was included in order to produce a graded response⁵². For the Ery-inducible
114 system, the ribosome methylase *ery^R* was included to confer resistance to Ery⁵³.

115 Rational mutations were made to improve some sensors prior to performing the direction
116 evolution experiments. Multiple versions of each sensor, each with different a promoter and RBS used to
117 drive the expression of the regulator, were tested (Supplementary Figure 3). The version with the largest
118 dynamic range was chosen for further optimization. Then, a number of potential improvements gleaned
119 from the literature or rationally designed were evaluated, the results of which are shown in
120 Supplementary Figure 4. After this step, we reduced the set of sensors to 14, removing copper, glucaric
121 acid and paraquat inducible systems because their responses were too small for subsequent optimization.
122 The response functions of the initial sensors are shown in Figure 2 (grey curves). Each function was
123 obtained by fitting the experimental data to the equation

124
$$y = y_{min} + (y_{max} - y_{min}) \frac{x^n}{K^n + x^n}, \quad (1)$$

125 where y is the promoter activity in RPU, x is the concentration of the small molecule, y_{min} is the leakiness,
126 y_{max}/y_{min} is the dynamic range, K is the sensitivity, and n is the cooperativity. The raw data points, including
127 error bars, used for this fit are shown in Supplementary Figure 5. While they all show some response, the
128 high leakiness, low dynamic range and low sensitivity are apparent for many. Of the 14, the aTc- and OC6-
129 sensors produced a good enough response to not require additional optimization (Table 1).

130 The remaining 12 were then subjected to directed evolution using the dual selection (Figure 1c,
131 Supplementary Figure 6). For each sensor, a library was constructed and cloned upstream of the operon
132 containing PheS and DNAP (Figure 1a) on a dual selection plasmid. The initial library contained a mixture
133 of random and rational mutations. For a subset of sensors, the output promoter was mutagenized:
134 selected bases in the -10 box and -35 box were randomized. To control regulator expression, critical
135 bases in the ribosome binding site (RBS) were randomized. For LacI and AraC, we partially mutagenized
136 key amino acid residues based on prior work^{23, 33-34}. Specifically, the genes were PCR amplified with
137 primers of limited degeneracy (*e.g.*, VNA, WKK, or NDC) thus allowing LacI Q18, F161, W220, Q291, and
138 L296 and AraC L133, E165, E169, and C280 to sample a subset of possible amino acids (Methods). The
139 specific mutations made to the initial library for each sensor are shown in Supplementary Appendix 2.

140 Multiple rounds of the dual selection were performed with the initial library. Between 4 and 23
141 rounds were performed, depending on how many issues needed to be corrected for each sensor.
142 Different interventions were performed during each round to bias solutions to address problems
143 identified for each sensor. The conditions for each round are presented in detail in Supplementary
144 Appendix 2. Typically, the stringency of the negative selection was increased at a particular round by
145 increasing the concentration of Cl-Phe from 2 mM to 4 mM. This biases against leakiness in the absence
146 of inducer. During positive selection, inducer was added to the surviving cells, leading to the expression
147 of DNAP. During early rounds, the maximum amount of inducer was added. For some sensors, we sought
148 to increase the sensitivity of the response by reducing the amount of inducer after each round; for
149 example, BetI was induced with 1 mM Cho in the final round of selection, down from 5 mM Cho in the
150 first round. After induction, the cells were encapsulated, lysed, and PCR amplified using the DNAP
151 expressed by the sensor (Methods). In early rounds, additional random mutations throughout the sensor
152 were introduced by using the PK6 DNAP during the positive selection (yielding an average of 1-2 mutations
153 per kilobase). In later rounds, the stringent KOD DNAP was used to reduce the diversity in the population.
154 After the amplification step of the positive selection, the constructs were recloned into the selection
155 plasmid. Recloning allows the selection plasmid to be reset each round, thus preventing the accumulation
156 of cheaters, and offers the opportunity to change the DNAP as needed. In some cases, in an effort to

157 combine multiple beneficial mutations into a single variant, gene shuffling⁵⁴ was used between rounds
158 (Methods).

159 During the selection rounds, additional interventions were included in order to reduce crosstalk
160 between systems. For example, crosstalk between the IPTG- and Ara- sensors is well known, where IPTG
161 reduces the output of the AraC/P_{BAD} system²³ (Supplementary Figure 7). To identify mutants that reduce
162 this, 1000 μ M IPTG was included during all rounds of selection for the Ara sensor. IPTG was also included
163 in the negative selection to prevent the evolution of an IPTG-induced AraC mutant. Crosstalk between
164 Van and DHBA was also observed and eliminated through the negative selection (Figure 2b,
165 Supplementary Figure 8). Salicylate was also found to antagonize the Cuma sensor (Figure 2c,
166 Supplementary Figure 7) and cross react with the DAPG sensor (Figure 2b, Supplementary Figure 8) and
167 was thus added to both the positive and negative selections.

168 After all of the rounds of selection are complete, the library was assembled into a YFP screening
169 plasmid (Supplementary Figure 6). Several clones were picked and assayed for output expression in the
170 presence and absence of inducer (Supplementary Appendix 2). In addition, when selecting against
171 crosstalk, the clones were screened for induction by these molecules. The mutants showing highest
172 improvement (leakiness, sensitivity, dynamic range, and orthogonality) were identified and sequenced
173 (Supplementary Appendix 2). Based on the mutations observed, one or more consensus sequences were
174 constructed and re-screened to identify the best variant. The final sequences of the evolved sensors,
175 including the mutations identified are provided in Supplementary Table 4. Mutations were identified
176 throughout the sensors, including the promoter/RBS controlling regulator expression, synonymous and
177 non-synonymous mutations throughout the regulator genes, and mutations/substitutions in the output
178 promoters (Figure 2a). On average, about eight cumulative mutations were made to each sensor as a
179 result of the rounds of dual selection.

180 The improvements in the response functions are shown in Figure 2a (blue curves). The fit
181 parameters to Equation 1 are provide in Table 1 (raw data are provided in Supplementary Figure 5). There
182 is marked improvement in many of the response functions, sometimes showing orders of magnitude
183 changes in the leakiness, dynamic range, and sensitivity. The Ery- and Acu- sensors showed slight
184 improvements in their response functions, but were not chosen to be part of the final set because of their
185 low dynamic range.

186 CymR, NahR, VanR, PhIF, and PcaU each responds to a substituted benzene. Therefore, we
187 examined the activity of this set of sensors against all five inducers. The optimized sensors showed
188 significant reduction in the crosstalk while maintaining high activity with their cognate inducer (Figure 2b,

189 Supplementary Figure 8). Improvements in the antagonism between CymR and Sal were also tested
190 (Figure 2c, Supplementary Figure 7). In the presence of 100 μ M Sal, the ability for Cuma to induce its
191 sensor drops by 1200-fold. The sensor obtained by rounds of positive selection in the presence of Cuma
192 reduces this by two orders of magnitude. There is also slight antagonism of AraC by IPTG, which also
193 improved as a result of the selection (Supplementary Figure 7). Collectively, these improvements allow
194 for all of these sensors to be used simultaneously in a single cell.

195 The best 12 sensors were then combined to form a “sensor array” that was inserted into the
196 genome of *E. coli* MG1655 to create “Marionette-Wild” (Figure 3 and Supplementary Table 6). Genomic
197 insertion has several benefits: it stabilizes the cluster and simplifies the use of multiple systems without
198 building large plasmids containing the regulators. The array consists of the 12 regulatory genes and *araE*
199 transporter organized into several operons (Figure 3a and Supplementary Figure 9). The genes were
200 organized into three operons controlled by three medium-strength constitutive promoters. Each gene is
201 encoded by its own ribosome binding site (RBS), which was rationally designed using the RBS Calculator⁵⁵
202 in order to achieve equivalent expression as when encoded on the plasmid (Methods and Supplementary
203 Figure 10). Strong terminators were included before and after the sensor array in order to insulate the
204 array from context effects. Phage transduction was used to move the sensor array to create two
205 additional cell lines: the *recA*-deficient *E. coli* DH10B strain for cloning “Marionette-Clo” and the protease-
206 deficient *E. coli* BL21 for protein expression “Marionette-Pro” (Methods).

207 The responses of the 12 genomically-encoded sensors in Marionette-Wild are shown in Figure 3b,
208 the parameters derived from the fits to Equation 1 are shown in Table 1, and the raw data points are
209 provided in Supplementary Figure 11 and Supplementary Appendix 1. Each response was measured by
210 transforming the strain with a p15a (Supplementary Figure 2) plasmid containing the output promoter
211 fused to YFP. Each response function shows at least 100-fold induction with similar levels of on- and off-
212 states. The technical information for the use of each sensor is organized as a series of datasheets in the
213 Supplementary Information. The response of each sensor was also measured in Marionette-Clo and
214 Marionette-Pro (Supplementary Appendix 1). The performances of the sensors closely match that of
215 Marionette-Wild with several exceptions; notably, the responses to IPTG (P_{Tac}) and choline (P_{Bet1}) are
216 leakier.

217 All of the sensors follow similar induction dynamics, with induction after 15 minutes and full
218 induction by 2 hours. Interestingly, those sensors based on activators were slower to turn on, as
219 compared to those based on repressors (Supplementary Figure 12). There is little cross reactivity from
220 the non-cognate inducers (Figure 3c and Supplementary Figure 13). The response functions for three

221 different promoters were also measured in the presence of the maximum levels of all 11 other inducers,
222 and there was little change in dynamic range (Supplementary Figure 14). The sensor responses were
223 measured during exponential growth. To evaluate performance in stationary phase, cells were grown
224 overnight (~20 hours) and response functions were measured (Methods). The responses closely match
225 those measured during exponential growth, with several exceptions (Supplementary Figure 12). Induction
226 on plates where the inducers are added to LB-agar resulted in similar responses as those observed in early
227 stationary phase (Supplementary Figure 15).

228 We tested whether carrying the sensor array impacts the growth rate of the three Marionette
229 strains (Supplementary Figure 16). The Marionette-Wild strain grows with a doubling time of 29.0 ± 1.9
230 min as compared 27.1 ± 1.2 for wild-type *E. coli* MG1655 (Methods). The other two Marionette strains
231 grow slightly faster, albeit within error (Supplementary Figure 16). Growth of Marionette-Wild was also
232 evaluated in the presence of all 12 inducers at maximum levels and only a modest effect was observed
233 (Supplementary Figure 16).

234 Carrying the sensor array requires the continuous expression of 12 regulatory proteins and a
235 transporter. This could lead to a draw on cellular resources that confers a selective advantage to
236 eliminating the array. While genomic insertion improves evolutionary stability^{21, 56-57}, it could still be
237 disrupted over time, particularly for the *recA*-positive⁵⁸ Marionette-Wild. To address this, we performed
238 three independent experiments to assess the evolutionary stability of Marionette-Wild. First, we
239 determined whether Marionette could reliably control a plasmid based promoter, even after extended
240 passage. The 12 reporter strains were passaged for 14 days in liquid culture without inducer, diluting the
241 cells 10^6 -fold each day (10^{84} -fold dilution total). On each day, a subset of cells from each line were grown
242 and assayed with and without inducer (Figure 3d and Supplementary Figure 17). Second, the Marionette-
243 Wild strain was passaged for nine days, streaking cultures on agar plates and inoculating single colonies
244 into liquid culture each day. On the tenth day, the culture was transformed with each of the 12 reporter
245 plasmids and assayed with and without the cognate inducer for each reporter. Third, we determined if
246 serial transfer would lead to the emergences of subpopulations⁵⁹. We passaged the Marionette-Wild
247 strain for nine days in liquid culture, diluting the cells 10^6 -fold each day (10^{54} -fold dilution total). On the
248 tenth day, the culture was transformed with each of the 12 reporter plasmids and assayed with and
249 without the cognate inducer for each reporter. For all three evolution experiments, the sensors perform
250 indistinguishably after growth and passaging (Supplementary Figure 17). There is no decline in the fold-
251 induction over time and there was no emergence of “broken” subpopulations by flow cytometry
252 (Supplementary Figure 18).

253 This work represents a dramatic expansion in our ability to study and control genes in cells. The
254 Marionette strains enable the modular control of up to 12 genes, simply by placing each one under the
255 control of a small (50 to 289 base pair) inducible promoter. This means that a single construct can be built
256 and then the expression levels perturbed in many ways through the combination of different small
257 molecules. This could be to determine the role of proteins in a natural system, picking apart the
258 stoichiometric requirements for a molecular machine⁶⁰⁻⁶¹. This can also be part of rapid optimization of
259 metabolic pathways, where the ideal stoichiometry can be identified without the need to build megabase-
260 scale libraries⁶²⁻⁶³. Through the use of CRISPRi⁶⁴, sRNA⁶⁵, or other tools, endogenous genes can be inducibly
261 down-regulated as well as up-regulated, thus enabling exquisite control of natural processes and
262 metabolic flux. Further, dynamic systems can be probed by controlling the timing of the induction of each
263 component in order to determine the role of ordered gene expression^{15, 66}. The ability to control gene
264 expression has been a major limitation in genetic engineering; now, pulling the strings on Marionette
265 enables unprecedented genetic control.

266

267 **Acknowledgements**

268

269 Supported by U.S. Office of Naval Research Multidisciplinary University Research Initiative grant #
270 N00014-16-1-2388 (AJM, THSS, and CAV). We would like to thank Aditya M. Kunjapur and Kristala L. J.
271 Prather for providing DNA templates for the amplification of P_{Van} , P_{3B5} , *vanR*, and *pcaU*.

272

273 **Accession**

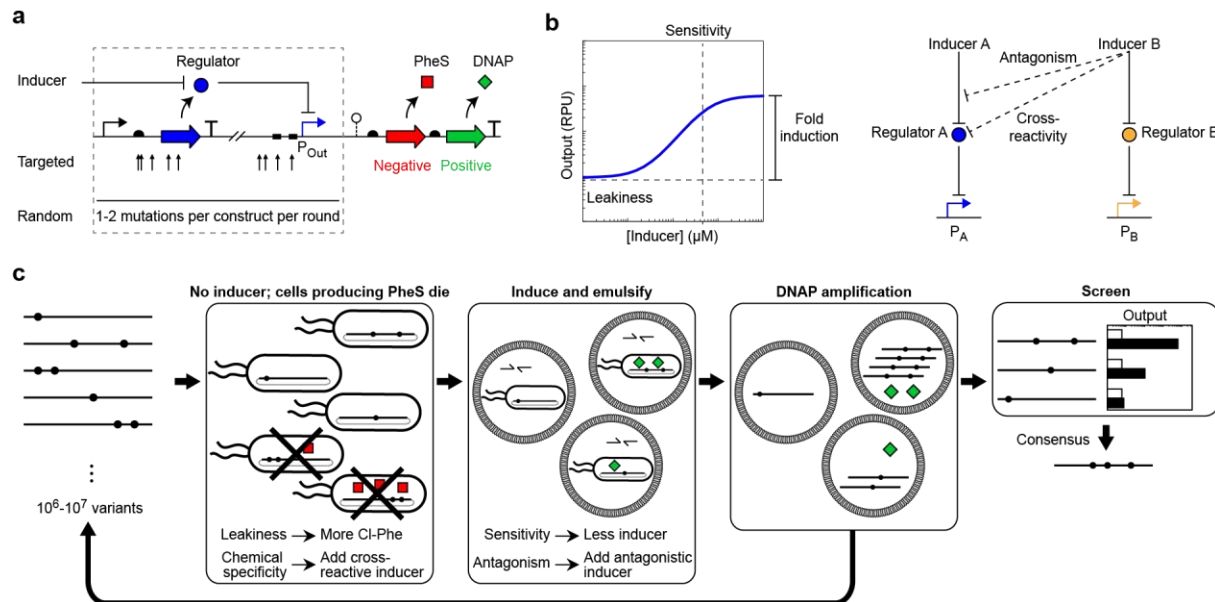
274 The following plasmids and strains can be acquired from Addgene: pAJM.711 (P_{PhIF} -YFP) 108512;
275 pAJM.712 (P_{CymRC} -YFP) 108513; pAJM.713 (P_{LuxB} -YFP) 108514; pAJM.714 (P_{VanCC} -YFP) 108515; pAJM.715
276 (P_{Tac} -YFP) 108516; pAJM.717 (P_{Tet^*} -YFP) 108517; pAJM.716 (P_{BAD} -YFP) 108518; pAJM.718 (P_{BetI} -YFP)
277 108519; pAJM.719 (P_{Ttg} -YFP) 108520; pAJM.1459 (P_{3B5C} -YFP) 108521; pAJM.721 (P_{SalITC} -YFP) 108522;
278 pAJM.944 (P_{Cin} -YFP) 108523; pAJM.847 ($PhIF^{AM}$ + P_{PhIF} -YFP) 108524; pAJM.657 ($CymR^{AM}$ + P_{CymRC} -YFP)
279 108525; pAJM.474 ($LuxR$ + P_{LuxB} -YFP) 108526; pAJM.773 ($VanR^{AM}$ + P_{VanCC} -YFP) 108527; pAJM.336 ($LacI^{AM}$
280 + P_{Tac} -YFP) 108528; pAJM.011 ($TetR$ + P_{Tet^*} -YFP) 108529; pAJM.677 ($AraC^{AM}$ + $AraE$ + P_{BAD} -YFP) 108530;
281 pAJM.683 ($BetI^{AM}$ + P_{BetI} -YFP) 108531; pAJM.661 ($TtgR^{AM}$ + P_{Ttg} -YFP) 108532; pAJM.690 ($PcaU^{AM}$ + P_{3B5B} -
282 YFP) 108533; pAJM.771 ($NahR^{AM}$ + P_{SalITC} -YFP) 108534; pAJM.1642 ($CinR^{AM}$ + P_{Cin} -YFP) 108535; pAJM.884
283 ($AcuR^{AM}$ + P_{Acu} -YFP) 108536; pAJM.969 ($MphR^{AM}$ + $EryR$ + P_{Mph} -YFP) 108537; sAJM.1504 (Marionette-Clo)
284 108251; sAJM.1505 (Marionette-Pro) 108253; sAJM.1506 (Marionette-Wild) 108254.

285

286 **Author contributions**

287 A.J.M and C.A.V. conceived the study and designed the experiments; A.J.M performed the experiments;
288 A.J.M and T.H.S.S. analyzed the data; A.J.M and C.A.V. wrote the manuscript with input from all the
289 authors.

290

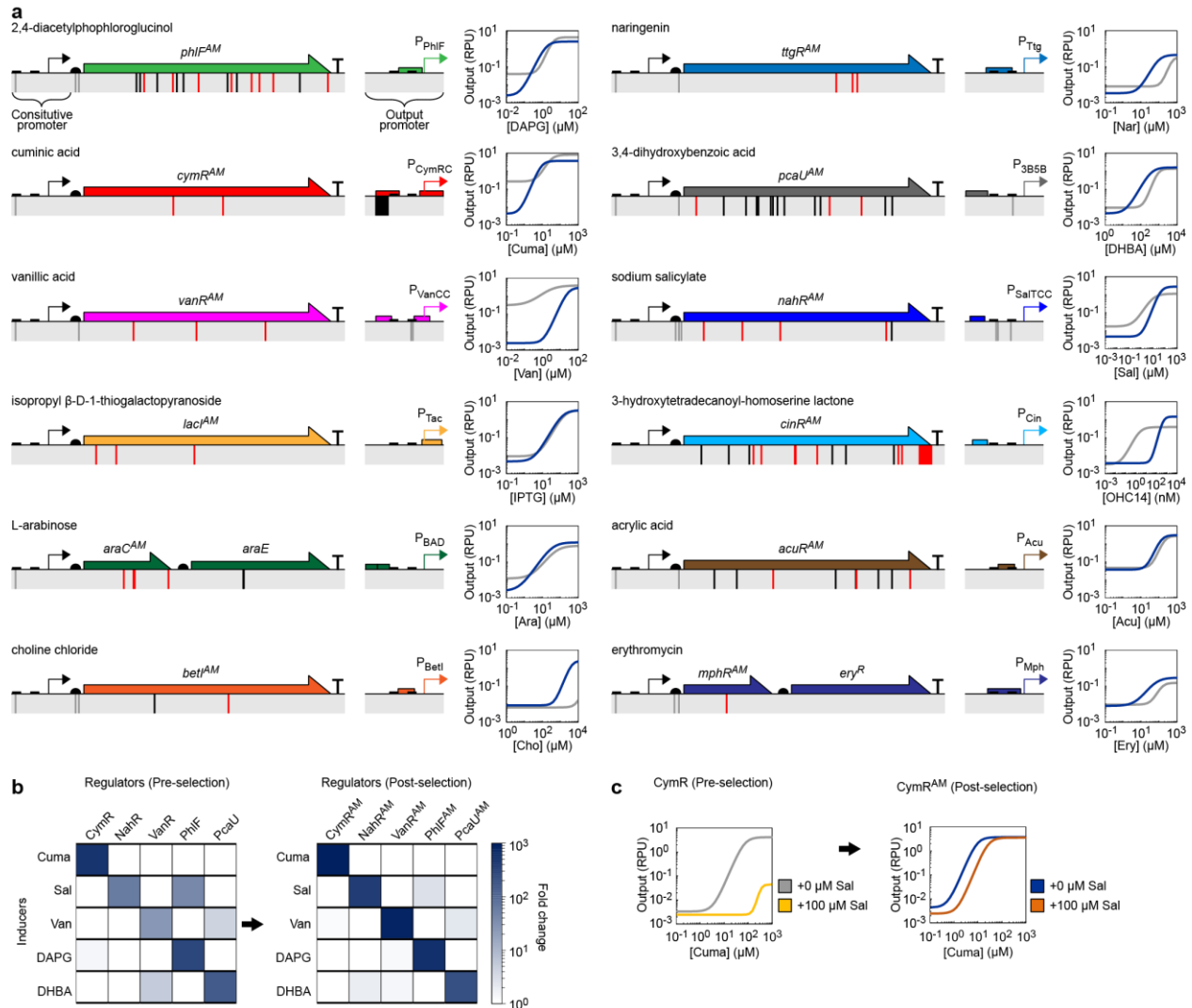


291

292

293 **Figure 1: A dual selection for sensor optimization.** **a)** A regulator (blue circle) is expressed from a weak
 294 constitutive promoter and controls expression from the output promoter (P_{Out}) while itself being
 295 controlled by an externally applied inducer molecule. Transcription from P_{Out} determines the expression
 296 level of an aminoacyl-tRNA synthetase (PheS; red square) and a DNA polymerase (KOD or PK6; green
 297 diamond). Initial libraries may contain targeted degeneracy in the regulator RBS, regulator CDS, or P_{Out}
 298 (arrows), and random mutations are added throughout the entire library during each round of selection.
 299 **b)** A response function captures the activity of P_{Out} at various levels of inducer. Regulator A affects
 300 promoter A, and is itself affected by inducer A. Inducer B may affect Regulator A (chemical cross-reactivity)
 301 or interfere with inducer A's action (antagonism). **c)** The dual selection schema is shown (see text for
 302 details). Dots denote mutations; half arrows represent PCR primers.

303

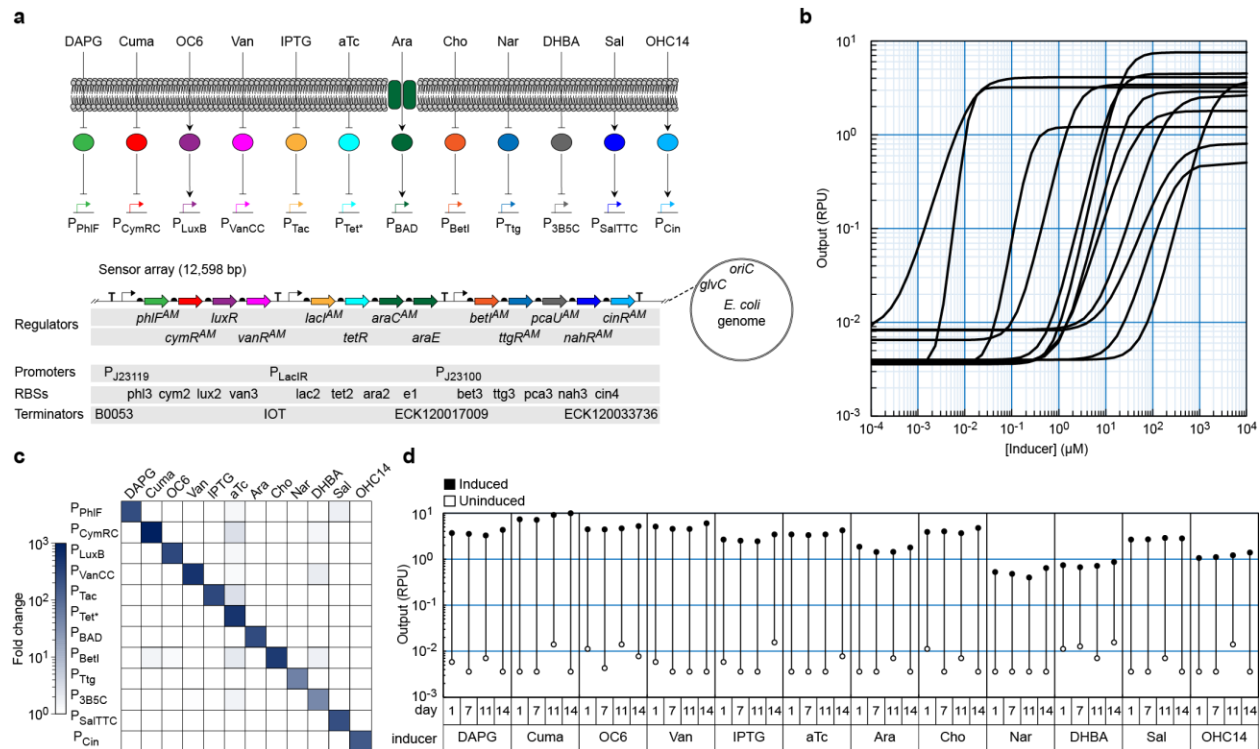


304
305

306 **Figure 2: Improved sensor performance.** **a)** Each genetically encoded sensor is shown, with coding (red)
 307 and non-coding (grey/black) mutations noted. Mutations in grey were also applied to the parental sensor.
 308 The corresponding response functions comparing the evolved (blue) and parental (grey) sensors. The fit
 309 of Equation 1 to the mean of three replicates performed on different days is shown (see Supplementary
 310 Figure 5 for data). The response function parameters for evolved sensors are provided in Table 1. **b)**
 311 Chemical cross-reactivity heat-map of reference (left) and evolved (right) sensors. Inducer concentrations
 312 were: 100 μM Cuma, 100 μM Sal, 100 μM Van, 10 μM DAPG, and 1 mM DHBA. The mean of three
 313 replicates performed on different days is shown (see Supplementary Figure 8 for data). **c)** Response
 314 function with Sal (light/dark orange) and without Sal (grey/blue) for parental CymR (left) and evolved
 315 CymRAM (right). The fit of Equation 1 to the mean of three replicates from different days is shown (see
 316 Supplementary Figure 7 for data). Sequences of promoters and regulators are provided in Supplementary
 317 Table 1 and 4.

318

319



320

321

322 **Figure 3: Marionette-Wild performance.** **a)** The molecular and genetic schematic of the Marionette
 323 cluster and its location in the *E. coli* genome. The cluster was inserted in the direction of leading strand
 324 replication, between 3,860,010 and 3,861,627 in *E. coli* MG1655 (NCBI accession number NC_000913),
 325 between 3,957,594 and 3,959,211 in *E. coli* DH10B (NC_010473), and between 3,720,027 and 3,721,644
 326 in *E. coli* BL21 (CP010816). **b)** Overlaid response functions for each of the 12 output promoters with their
 327 cognate inducers. The fit of Equation 1 to the mean of three replicates performed on different days is
 328 shown (see Supplementary Figure 11 for data). The response function parameters are provided in Table
 329 1. **c)** Chemical cross-reactivity heat-map of the 12 output promoters with each inducer. Inducer
 330 concentrations were: 25 μ M DAPG, 500 μ M Cuma, 10 μ M OC6, 100 μ M Van, 1 mM IPTG, 200 nM aTc, 4
 331 mM Ara, 10 mM Cho, 1 mM Nar, 2.5 mM DHBA, 250 μ M Sal, and 10 μ M OHC14. The mean of three
 332 replicates performed on different days is shown (see Supplementary Figure 13 for data). **d)** Output of
 333 uninduced (open circles) and induced (closed circles) cultures on day 1, 7, 11, and 14 days of passaging.
 334 Inducer concentrations were: 25 μ M DAPG, 500 μ M Cuma, 10 μ M OC6, 100 μ M Van, 1 mM IPTG, 200 nM
 335 aTc, 4 mM Ara, 10 mM Cho, 1 mM Nar, 2.5 mM DHBA, 250 μ M Sal, and 10 μ M OHC14. A single
 336 evolutionary trajectory is shown. Passaging details and data from other days are provided in
 337 Supplementary Figure 17.

338

339 **Table 1. Sensor response function parameters^a**

Inducer ^d	Max inducer (μM) ^b	Genome-based regulator (Marionette-Wild ^c)				Plasmid-based regulator (<i>E. coli</i> DH10B)				
		Y_{max} (RPU)	Y_{min} (RPUx10 ³)	K (μM)	n	Y_{max} (RPU)	Y_{min} (RPUx10 ³)	K (μM)	n	
DAPG	2,4-Diacetylphosphoroglucinol	25	3.4	6.5	2.1	2.3	2.5	2.5	1.7	2.1
Cuma	Cuminic acid	100	7.6	3.6	22	2.3	3.7	4.3	8.9	2.4
OC6	3OC6-AHL	10	4.1	8.6	0.012	1.7	1.3	2.4	0.12	1.8
Van	Vanillic acid	100	4.5	4.0	14	2.1	3.0	2.4	26	2.3
IPTG	Isopropyl-beta-D-thiogalactoside	1000	2.6	8.3	190	1.7	3.3	4.8	140	1.8
aTc	Anhydrotetracycline HCl	0.2	3.2	3.6	0.012	4.4	2.4	4.9	0.013	3.8
Ara	L-Arabinose	4000	1.8	3.6	43	1.7	1.2	2.4	37	1.5
Cho	Choline chloride	10000	3.7	4.0	1900	2.0	2.6	8.5	4100	2.7
Nar	Naringenin	1000	0.5	4.0	280	2.3	0.5	3.4	95	1.9
DHBA	3,4-Dihydroxybenzoic acid	1000	0.8	8.0	240	1.5	1.6	4.5	370	1.8
Sal	Sodium salicylate	100	2.9	3.8	29	2.1	2.8	4.7	43	1.8
OHC14	3OHC14:1-AHL	10	1.2	3.6	0.25	3.0	1.5	3.0	0.43	2.3
Acu	Acrylic acid	1000					3.1	37.0	130	2.5
Ery	Erythromycin	125					0.3	8.0	65	1.5

- 340 a. Response data from at least days were averaged and fit to Equation 1 (Methods). Full response functions are provided in Supplementary Appendix 1.
 341 b. Growth defects are observed above this concentration.
 342 c. Based on *E. coli* MG1655. Data for Marionette-Clo (DH10B) and Marionette-Pro (BL21) are provided in Supplementary Appendix 1.
 343 d. DAPG-Santa Cruz sc-206518; Cuma-Sigma 268402; OC6-Sigma K3007; Van-Sigma 94770; IPTG-Gold I2481C25; aTc-Sigma 37919; Ara-Sigma A3256; Cho-
 344 Sigma C7017; Nar-Sigma N5893; DHBA-Sigma 37580; Sal-Sigma S3007; OHC14-Sigma 51481; Acu-Sigma 147230; Ery-Sigma E5389.

345

346

347 **Methods**

348 **Strains, plasmids, and media.** *Escherichia coli* DH10B (New England Biolabs, Ipswich, MA – USA) was used
349 for all routine cloning and directed evolution. Plasmid-based regulator systems were characterized in *E.*
350 *coli* DH10B. Marionette-Wild, -Clo, and -Pro were derived from *E. coli* MG1655⁶⁷, *E. coli* DH10B, and *E.*
351 *coli* BL21 (New England Biolabs, Ipswich, MA – USA) cells respectively. *E. coli* JTK164H was used to clone
352 RK6 suicide vectors⁶⁸. All other plasmids contain p15A origins of replication and kanamycin resistance
353 (Supplementary Figures 2 and 6). LB-Miller media (BD, Franklin Lakes, NJ - USA) was used for directed
354 evolution, stability assays, and cytometry assays unless specifically noted. 2xYT liquid media (BD, Franklin
355 Lakes, NJ - USA) and LB + 1.5% agar (BD, Franklin Lakes, NJ – USA) plates were used for routine cloning
356 and strain maintenance. M9 media (1x M9 Salts [Millipore Sigma, St. Louis, MO - USA], 2 mM MgSO₄, 100
357 μM CaCl₂, and 0.2% Casamino acids) supplemented with either 0.4% glucose or 0.4% glycerol was used
358 for cytometry assays where noted.

359
360 **Chemical transformation.** For routine transformations, strains were made competent for chemical
361 transformation. Overnight cultures (250 μl for *E. coli* DH10B derived cells, 100 μl for *E. coli* MG1655 and
362 BL21 derived cells) were subcultured into 100 ml SOB media (BD, Franklin Lakes, NJ – USA) and grown at
363 37 °C, 250 rpm for 3 hours. Cultures were centrifuged (4500g, 4 °C, 10 minutes) and pellets were
364 resuspended in 15 ml TFBI buffer⁵¹ (30 mM KOAc, 50 mM MnCl₂, 100 mM RbCl, 10 mM CaCl₂, and 15% v/v
365 glycerol, pH 5.0). After 1 hour on ice, cells were centrifuged (4500g, 4 °C, 10 minutes) and pellets were
366 resuspended in 2 ml TFBII buffer (10 mM NaMOPS pH 7.0, 75 mM CaCl₂, 10 mM RbCl, and 15% v/v
367 glycerol). Competent cells were stored at -80 °C until use.

368
369 **Response function measurements (mid-log phase).** All measurements shown were taken by cytometry
370 of cells in mid-log growth except when noted. Glycerol stocks of strains containing the plasmids of interest
371 were streaked on LB + 1.5% Agar plates and grown overnight at 37 °C. Single colonies were inoculated
372 into 1 ml LB + antibiotics in 2-ml 96-deepwell plates (USA Scientific, Orlando, FL - USA) sealed with an
373 AeraSeal film (Excel Scientific, Victorville, CA - USA) and grown at 37 °C, 900 rpm overnight in a Multitron
374 Pro shaker incubator (INFORS HT, Bottmingen, Switzerland). The overnight growths were diluted 1:200
375 into 1 ml LB + antibiotics in 2-ml 96-deepwell plates + AeraSeal film and grown at 37 °C, 900 rpm. After 2
376 hours the growths were diluted (*E. coli* DH10B/Marionette-Clo 1:500; *E. coli* BL21/Marionette-Pro 1:2,000;
377 *E. coli* MG1655/Marionette-Wild 1:5,000) into prewarmed LB + antibiotics + inducer where necessary in

378 2-ml 96-deepwell plates + AeraSeal film and grown at 37 °C, 900 rpm for 5 hours. After growth, 20 µl of
379 culture sample was diluted into 180 µl PBS + 200 µg/ml kanamycin to inhibit translation.

380
381 **Response function measurements (stationary phase).** Measurements were taken from cells in stationary
382 phase to generate data shown in Supplementary Appendix 1 and Supplementary Figures 12 and 13.
383 Glycerol stocks of strains containing the plasmids of interest were streaked on LB + 1.5% Agar plates and
384 grown overnight at 37 °C. Single colonies were inoculated into 1 ml LB + antibiotics in 2-ml 96-deepwell
385 plates (USA Scientific, Orlando, FL - USA) sealed with an AeraSeal film (Excel Scientific, Victorville, CA -
386 USA) and grown at 37 °C, 900 rpm overnight in a Multitron Pro shaker incubator (INFORS HT, Bottmingen,
387 Switzerland). The overnight growths were diluted 1:200 into 1 ml LB + antibiotics in 2-ml 96-deepwell
388 plates + AeraSeal film and grown at 37 °C, 900 rpm. After 2 hours the growths were diluted (*E. coli*
389 DH10B/Marionette-Clo 1:500; *E. coli* BL21/Marionette-Pro 1:2,000; *E. coli* MG1655/Marionette-Wild
390 1:5,000) into prewarmed LB + antibiotics + inducer where necessary in 2-ml 96-deepwell plates + AeraSeal
391 film and grown at 37 °C, 900 rpm for 20 hours. After growth, 2 µl of culture sample was diluted into 198
392 µl PBS + 200 µg/ml kanamycin to inhibit translation.

393
394 **Time course (mid-log phase).** For Supplemental Figure 12: mid-log induction time course, glycerol stocks
395 of strains containing the plasmids of interest were streaked on LB + 1.5% Agar plates and grown overnight
396 at 37 °C. Single colonies were inoculated into 1 ml LB + antibiotics in 2-ml 96-deepwell plates (USA
397 Scientific, Orlando, FL - USA) sealed with an AeraSeal film (Excel Scientific, Victorville, CA - USA) and grown
398 at 37 °C, 900 rpm overnight in a Multitron Pro shaker incubator (INFORS HT, Bottmingen, Switzerland).
399 The overnight growths were diluted 1:200 into 1 ml LB + antibiotics in 2-ml 96-deepwell plates + AeraSeal
400 film and grown at 37 °C, 900 rpm. After 2 hours the growths were diluted 1:500 into prewarmed LB +
401 antibiotics. After 0, 1, 2, 3, 3.5, 4, 4.25, 4.5, or 4.75 hours, cultures were further diluted 1:10 into
402 prewarmed LB + antibiotics + inducer where necessary in 2-ml 96-deepwell plates + AeraSeal film and
403 grown at 37 °C, 900 rpm for 5, 4, 3, 2, 1.5, 1, 0.75, 0.5, or 0.25 hours (5 hours total after the initial growth).
404 After growth, 20 µl of culture sample was diluted into 180 µl PBS + 200 µg/ml kanamycin to inhibit
405 translation.

406
407 **Time course (mid-log phase to stationary phase).** For Supplemental Figure 12: mid-log to stationary
408 induction time course, glycerol stocks of strains containing the plasmids of interest were streaked on LB
409 + 1.5% Agar plates and grown overnight at 37 °C. Single colonies were inoculated into 1 ml LB + antibiotics

410 in 2-ml 96-deepwell plates (USA Scientific, Orlando, FL - USA) sealed with an AeraSeal film (Excel Scientific,
411 Victorville, CA - USA) and grown at 37 °C, 900 rpm overnight in a Multitron Pro shaker incubator (INFORS
412 HT, Bottmingen, Switzerland). The overnight growths were diluted 1:200 into 1 ml LB + antibiotics in 2-ml
413 96-deepwell plates + AeraSeal film and grown at 37 °C, 900 rpm. After 2 hours the growths were diluted
414 1:5000 into prewarmed LB + antibiotics + inducer where necessary in 2-ml 96-deepwell plates + AeraSeal
415 film and grown at 37 °C, 900 rpm for 5, 6, 7, 8, 9, 10, or 20 hours. After growth, 2 to 20 µl of culture
416 sample was diluted into 180-198 µl PBS + 200 µg/ml kanamycin to inhibit translation.

417
418 **Cytometry analysis.** Fluorescence characterization with cytometry was performed on a BD LSR Fortessa
419 flow cytometer with HTS attachment (BD, Franklin Lakes, NJ - USA). Cells diluted in PBS + kanamycin were
420 run at a rate of 0.5 µl/s. The events were gated by forward scatter height (mid-log: 1,000-10,000;
421 stationary: 500-5000) and side scatter area (mid-log: 1,000-10,000; stationary: 500-5,000) to reduce false
422 events. After gating, thousands of events were used for analysis. For each sample, the median YFP
423 fluorescence was calculated. All output values are reported in terms of relative promoter units (RPU). For
424 a given promoter measurement, the strain (*E. coli* DH10B, Marionette-Wild, etc) is transformed with the
425 plasmid. The strain is then assayed alongside a strain containing the RPU standard plasmid
426 (Supplementary Figure 1, Supplementary Table 8) as well as an autofluorescence control. The median
427 autofluorescence value is subtracted from the all other median fluorescence values, including that of the
428 RPU standard. The experimental sample value is then divided by the RPU standard value.

429
430 **Library generation.** Portions of the initial libraries were created by PCR using degenerate oligonucleotides
431 (Integrated DNA Technologies Coralville, IA - USA). These fragments were joined into a degenerate, full-
432 length sensor module by overlap PCR. Sensor modules were assembled into selection vectors by Golden
433 Gate assembly⁷⁰. Linear insert and plasmid selection vector were mixed at 1:1 molar ratio totaling ~ 1 µg
434 DNA along with 5 µl 10x T4 ligase Buffer, 1 µl T4 DNA ligase (2,000,000 U/ml), 2 µl BbsI (10,000 U/ml) (all
435 from New England Biolabs, Ipswich, MA - USA) in 50 µl total. Reactions were cycled 45 times between 2
436 minutes at 37 °C and 5 minutes at 16 °C, and then incubated for 30 minutes at 50 °C, 30 minutes at 37 °C,
437 and 10 minutes at 80 °C in a DNA Engine cycler (Bio-Rad, Hercules, CA – USA). An additional 1 µl BbsI was
438 then added, and the assembly was incubated for 1 hour at 37 °C. Assemblies were then purified using
439 Zymo Spin I columns (Zymo Research, Irvine, CA - USA). Host cells were transformed with library plasmid
440 by electroporation. Supplementary Appendix 2 contains a depiction of all degeneracy found in the “Initial
441 library” for each selection.

442

443 **Negative selection.** LB media + 8 mM Cl-Phe (4-Chloro-DL-phenylalanine [Millipore Sigma, St. Louis, MO
444 - USA]) was mixed, autoclaved, and stored at room temperature. Cl-Phe has a tendency to adhere to
445 glassware, and care was taken to avoid disturbing the water + LB powder + Cl-Phe powder mixture prior
446 to autoclaving. LB media + 8 mM Cl-Phe was mixed with plain LB media to achieve the desired
447 concentration of Cl-Phe (See Interventions:[Cl-Phe] for each selection in Supplementary Appendix 2).
448 Following transformation and outgrowth, cultures were diluted into 7 ml LB + Cl-Phe supplemented with
449 antibiotics as well as any cross-reactive inducers (See Interventions:[Negative ligand] for each selection in
450 Supplementary Appendix 2). Cultures were grown at 37 °C for 12-16 hours.

451

452 **Positive selection.** Following negative selection, cultures were diluted 1:100 into 2 ml LB + antibiotics in
453 culture tubes and grown at 37 °C, 250 rpm for 2 hours. The cultures were then diluted 1:100 into 2 ml
454 prewarmed LB + antibiotics + inducer (See Interventions:[Positive ligand] for each selection in
455 Supplementary Appendix 2) and grown at 37 °C, 250 rpm for 4 hours. Following induction, 1 ml of culture
456 was centrifuged at (5,000g, 25 °C, 10 minutes). Supernatant was removed and the cell pellet was
457 resuspended in 50 µl 1x CPR buffer (50 mM Tris-HCl pH 8.8, 10 mM KCl, 2 mM MgSO₄, 10 mM (NH₄)₂SO₄).
458 5 µl resuspension was added to 95 µl of 1 x CPR buffer plus 0.4 µM CPR primers and 200 µM dNTPs. This
459 aqueous phase added to a 2 ml centrifuge tube containing 438 µl Tegosoft DEC (Evonik, Essen, Germany),
460 42 µl AbilWE09 (Evonik, Essen, Germany) and 120 µl mineral oil (Millipore Sigma, St. Louis, MO - USA) and
461 the rubber stopped from a 1 ml syringe. The mixture was vortexed at maximum setting for 2 minutes.
462 The emulsion was split evenly five 0.2 ml PCR tubes, and thermal cycled (95 °C for 5 minutes; 20 cycles of
463 [95 °C for 30 seconds, 55 °C for 30 seconds, 72 °C for 2 minutes/kb]; and 72 °C for 5 min). Emulsions were
464 then centrifuged (10,000g, 25 °C, 10 minutes) and the upper (oil) phase was removed. Then, 100 µl H₂O
465 and 500 µl chloroform were added and the mixture was pipetted to disrupt the pellet. The resuspension
466 was then transferred to a 1.5 ml heavy-gel phase-lock tube (5 Prime, San Francisco, CA - USA) and
467 centrifuged (16,000g, 25 °C, 2 minutes). The upper (aqueous) phase was collected, and DNA was purified
468 using Zymo Spin I columns. The library was amplified in a recovery PCR using Accuprime *Pfx* and nested
469 recovery primers, gel purified, and assembled as described above. A depiction of the CPR primer and
470 recovery primer amplification are provided in Supplementary Figure 6.

471

472 **Library shuffling.** Between some rounds of selection (See Interventions:Notes for each selection in
473 Supplementary Appendix 2), libraries were shuffled upon themselves such that fragments of each mutant

474 mutually serve as both primer and template for a primer-less PCR amplification⁵⁴. 1 µg linear, library DNA
475 (from the recovery PCR) was added to a mild DNase reaction (500 mM Tris pH 7.4, 100 mM MnCl₂, 0.5 U
476 DNase [New England Biolabs, Ipswich, MA - USA]) and lightly digested for 3 minutes at 15 °C. Fragmented
477 DNA was purified using Zymo Spin I columns and reassembled in a primer-less PCR in 1 x KAPA HiFi Master
478 Mix (KAPA Biosystems, Wilmington, MA – USA) by thermal cycling (95 °C for 2 minutes; 35 cycles of [95 °C
479 for 30 seconds, 65 °C for 90 seconds, 62 °C for 90 seconds, 59 °C for 90 seconds, 56 °C for 90 seconds, 53
480 °C for 90 seconds, 50 °C for 90 seconds, 47 °C for 90 seconds, 44 °C for 90 seconds, 41 °C for 90 seconds,
481 68 °C for 90 seconds]; and 72 °C for 4 minutes). The reassembly was purified using Zymo Spin I columns,
482 reamplified using Accuprime *Pfx* and CPR primers, gel purified, and assembled as described above.

483
484 **On/off screen.** At the end of each selection, libraries were assembled into the YFP screening plasmid
485 (Supplementary Figure 6). Host cells were transformed and plated on LB-agar. Between 35 and 92
486 individual clones were picked and assayed by cytometry as described. Cells were grown with no inducer,
487 in the presence of cognate inducer, and when necessary in the presence of relevant non-cognate inducers.
488 Measurements were made of cells in mid-log phase by cytometry as described. The most promising
489 clones, as judged by dynamic range and orthogonality, were mini-prepped and the sensor region was
490 sequenced.

491
492 **Genomic integration.** In preparation of recombineering, cells were transformed with a plasmid
493 containing Ara-inducible λ Red recombination machinery with a temperature sensitive origin of
494 replication⁷¹. 50 µl of overnight culture was subcultured in 50 ml LB medium and grown at 30 °C, 250 rpm
495 for 2 hours. 2 mM Ara was added, and the culture continued to grow at 30 °C, 250 rpm for 3 hours. The
496 culture was then centrifuged (4500g, 4 °C, 10 minutes) and washed with ice cold 10% glycerol four times,
497 with the fourth resuspension in 200 µl 10% glycerol. Recombineering-ready cells were stored at -80 °C
498 until use. For the first insertion, six genes (*phlF^{AM}*, *cymR^{AM}*, *luxR*, *vanR^{AM}*, *lacI^{AM}*, and *tetR*) were Golden
499 Gate assembled using BsaI into an RK6 suicide vector (which needs Pir protein in order to propagate)⁶⁸.
500 Pir-expressing *E. coli* JTK164H cells were transformed, and plasmids were purified, verified, and linearized
501 with Bpil leaving homology to the *glvC* pseudogene. Recombineering-ready *E. coli* MG1655 cells were
502 electroporated and transformed with gel-purified, linearized inserts. After an outgrowth of one hour at
503 37 °C, transformations were plated on LB-agar plates + antibiotic (5 µg/ml chloramphenicol). Colonies
504 were picked and grown at 37°C in LB + antibiotic, and the presence of the insert was verified by colony
505 PCR. For the second insertion, this strain was made recombineering-ready and the process was repeated

506 with the next set of genes (*araC^{AM}*, *araE*, *betI^{AM}*, and *ttgR^{AM}*) with the insert containing homology to *tetR*
507 and *glvC* and conferring resistance to 20 µg/ml spectinomycin. For the third insertion, this strain was
508 made recombineering-ready and the process was repeated with the final set of genes (*pcaU^{AM}*, *nahR^{AM}*,
509 and *cinR^{AM}*) with the insert containing homology to *ttgR^{AM}* and *glvC* and conferring resistance to 5 µg/ml
510 chloramphenicol. See Supplementary Figure 9 for schematic details.

511
512 **Phage transduction to transfer the Marionette cluster.** 50 µl of overnight culture of Marionette-Wild
513 was subcultured in 5 ml LB medium + 0.2% glucose and 5 mM CaCl₂ and grown at 37 °C, 250 rpm for 30
514 minutes. 100 µl p1 phage lysate (10⁹ pfu/ml) was added and the culture was grown at 37 °C, 250 rpm
515 until lysis (3 hours)⁷². 50 µl chloroform was added and the culture continued at 37 °C, 250 rpm for 5
516 minutes. Culture was centrifuged (9200g, 25 °C, 10 minutes). Supernatant was filtered (0.45 µM) and
517 stored at 4 °C until use. 1.5 ml of overnight culture of *E. coli* MG1655, BL21, or DH10B (the DH10B cells
518 contained a temperature-sensitive plasmid transiently expressing RecA) was centrifuged (10,000g, 25 °C,
519 5 minutes). The cell pellet was resuspended in 750 µl P1 buffer (5 mM MgSO₄ and 10 mM CaCl₂) and up
520 to 100 µl Marionette-P1 phage lysate was added. After 30 minutes at 25 °C, 1 ml LB + 200 µl 1 M sodium
521 citrate was added and the culture was grown at 37 °C, 250 rpm for 30 minutes. The culture was
522 centrifuged (10,000g, 25 °C, 2 minutes) and the pellets were resuspended in 100 µl LB and plated on LB-
523 agar plates + 5 µg/ml chloramphenicol and 5 mM sodium citrate. Colonies were picked and grown at 37
524 °C in LB + 5 µg/ml chloramphenicol and 5 mM sodium citrate, and the presence of the insert was verified
525 by colony PCR. The entire Marionette cluster was verified by sequencing PCR amplicons of the cluster
526 from the genome of Marionette-Wild.

527
528 **Sensor induction on plates.** Cells were transformed with reporter plasmids and, following outgrowth at
529 37°C for one hour, plated on LB-agar (LB-Miller powder + 1.5 % agar [BD, Franklin Lakes, NJ – USA]) with
530 and without the appropriate inducer. After an overnight incubation at 37°C for 16 hours, plates were
531 incubated at 4°C for one hour and imaged using a ChemiDocMP Imaging system (Bio-Rad, Hercules, CA -
532 USA) and Image Lab 4.0 software (Bio-Rad, Hercules, CA - USA) employing blue epi illumination, a 530/28
533 filter and a 0.1 second exposure. Raw images were rotated and cropped using XnView (XnSoft, Reims,
534 France). Individual colonies were scraped from the plate, resuspended in 200 µl PBS + 200 µg/ml
535 kanamycin, and assayed by cytometry as described in Cytometry analysis.

536

537 **Plate reader assays to measure growth rates.** Glycerol stocks of strains of interest were streaked on LB +
538 1.5% Agar plates and grown overnight at 37 °C. Single colonies were inoculated into 1 ml LB in 2-ml 96-
539 deepwell plates (USA Scientific, Orlando, FL - USA) sealed with an AeraSeal film (Excel Scientific, Victorville,
540 CA - USA) and grown at 37 °C, 900 rpm overnight in a Multitron Pro shaker incubator (INFORS HT,
541 Bottmingen, Switzerland). The overnight growths were diluted 1:200 into 1 ml LB in 2-ml 96-deepwell
542 plates + AeraSeal film and grown at 37 °C, 900 rpm. After 2 hours the growths were diluted (*E. coli*
543 DH10B/Marionette-Clo 1:500; *E. coli* BL21/Marionette-Pro 1:2,000; *E. coli* MG1655/Marionette-Wild
544 1:5,000) into prewarmed LB + inducer where necessary in 2-ml 96-deepwell plates. 100 µl of this culture
545 was immediately transferred to a 300-µl 96-well black walled optical bottom plates (Thermo Scientific
546 Nunc, Waltham, MA – USA) sealed with a BreathEasy film (Sigma-Aldrich, St. Louis, MO – USA), and grown
547 in a Synergy H1 plate reader (BioTek, Winooski, VT – USA) at 37 °C, 1000 rpm. OD₆₀₀ was measured every
548 20 minutes over 12 hours of growth. OD₆₀₀ readings were also taken from wells containing media with no
549 cells, and for each time point, readings from such wells were subtracted from the appropriate sample
550 measurements to remove background. OD₆₀₀ values were converted to equivalent 1 cm path length
551 measurements using a standard curve.

552
553 **Calculation of growth rates.** To calculate doubling times, the last measurement with OD₆₀₀ < 0.1 and the
554 first measurement with OD₆₀₀ > 0.4 were identified, and the doubling time was calculated assuming
555 exponential growth between those two points. Doubling time is calculated as elapsed time (in minutes)
556 divided by the number of doublings that occurred in that time ($\log_2[\text{final OD}_{600}/\text{initial OD}_{600}]$).

557
558 **Evolutionary stability (passaging with reporters).** Marionette-Wild was transformed with each of the 12
559 reporter plasmids and plated on LB-agar. Single colonies were inoculated into 1 ml LB + antibiotics in 2-
560 ml 96-deepwell plates (USA Scientific, Orlando, FL - USA) sealed with an AeraSeal film (Excel Scientific,
561 Victorville, CA - USA) and grown at 37 °C, 900 rpm overnight in a Multitron Pro shaker incubator (INFORS
562 HT, Bottmingen, Switzerland). The overnight growths were diluted 1:200 into 1 ml LB + antibiotics in 2-ml
563 96-deepwell plates + AeraSeal film and grown at 37 °C, 900 rpm. After 2 hours, the growths were diluted
564 1:5000 into prewarmed LB + antibiotics + inducer where necessary in 2-ml 96-deepwell plates + AeraSeal
565 film and grown at 37 °C, 900 rpm for 5 hours. After growth, 20 µl of culture sample was diluted into 180
566 µl PBS + 200 µg/ml kanamycin to inhibit translation and assayed by cytometry as described in Cytometry
567 analysis. Uninduced cultures were allowed to grow at 37 °C overnight (17 hours) and the process
568 (beginning with the 1:200 dilution of the overnight culture) was repeated each day for 14 days.

569

570 **Evolutionary stability (passaging on plates).** A single colony of Marionette-Wild was inoculated into 1 ml
571 LB in 2-ml 96-deepwell plates (USA Scientific, Orlando, FL - USA) sealed with an AeraSeal film (Excel
572 Scientific, Victorville, CA - USA) and grown at 37 °C, 900 rpm for 12 hours in a Multitron Pro shaker
573 incubator (INFORS HT, Bottmingen, Switzerland). The overnight growth was streaked onto LB-agar plates
574 and grown at 37 °C for 12 hours. This process was repeated 9 times. The final culture was made
575 chemically competent as described in Chemical transformation, transformed with relevant reporter
576 plasmids, and assayed with cytometry as described in Cytometry analysis.

577

578 **Evolutionary stability (passaging in liquid culture).** A single colony of Marionette-Wild was inoculated
579 into 1 ml LB in 2-ml 96-deepwell plates (USA Scientific, Orlando, FL - USA) sealed with an AeraSeal film
580 (Excel Scientific, Victorville, CA - USA) and grown at 37 °C, 900 rpm for 12 hours in a Multitron Pro shaker
581 incubator (INFORS HT, Bottmingen, Switzerland). The overnight growths were diluted 1:200 into 1 ml LB
582 in 2-ml 96-deepwell plates + AeraSeal film and grown at 37 °C, 900 rpm. After 2 hours, the growths were
583 diluted 1:5000 into prewarmed LB in 2-ml 96-deepwell plates + AeraSeal film and grown at 37 °C, 900 rpm
584 for 22 hours. This process was repeated 9 times. The final culture was made chemically competent as
585 described in Chemical transformation, transformed with relevant reporter plasmids, and assayed with
586 cytometry as described in Cytometry analysis.

587

588 **Computational methods (fitting to the response function).** To parameterize the response function, error
589 minimization was performed using the Solver function in Excel software (Microsoft, Redmond, WA - USA).
590 Equation 1 was entered with y_{min} , y_{max} , K , and n as tunable parameters, x (inducer concentration) as the
591 independent variable and y as the output. For each x , the error between the measured RPU value and
592 the output of the function was determined. The total error was determined by summing the normalized
593 square of the error ($[y - \text{measured RPU value}]^2 / y$) for each x . The Solver function minimized the total error
594 by tuning y_{min} , y_{max} , K , and n .

595

596 **Computational methods (partial randomization of amino acids).** Initial libraries for the selection of LacI
597 and AraC utilized partial randomization of amino acids. Previous literature informed decisions regarding
598 the desirability of including each possible residue in the library. The CASTER 2.0 tool⁷³ was used to design
599 degenerate oligodeoxynucleotides that can sample the desired amino acids while limiting undesired
600 amino acids and stop codons.

601
602 **Computational methods (RBS design).** The initial RBS for each regulator in the Marionette cluster was
603 designed using the RBS Calculator v1.1⁵⁵ using the *E. coli* DH10B 16S rRNA setting. The “Pre-Sequence”
604 included the last 100 bp of the upstream CDS (where appropriate) as well as any scars used in Golden
605 Gate assembly. The “Target Translation Initiation Rates” were chosen based on the RBS strength of the
606 plasmid-based sensor (found using the “Reverse Engineer RBSs” tool) and compensating for the reduction
607 in copy number and increase in promoter strength associated with the move to the genomic system. After
608 initial assembly and testing, a decision was made based on the appearance of the response function as to
609 whether the RBS was too low, too high, or good. Low RBSs were rationally mutated to more closely
610 resemble the consensus Shine-Dalgarno sequence (TAAGGAGGT) while high RBSs were rationally mutated
611 to less closely resemble the consensus Shine-Dalgarno sequence. All rationally designed RBS variants
612 were checked using the “Reverse Engineer RBSs” to guard against making dramatic, unanticipated
613 changes to the RBS strength. Rational mutations are noted in Supplementary Table 2. Translation
614 Initiation Rate (in arbitrary units) for each RBS variant is provided in Supplementary Figure 10.

615 References

- 616 1. Zuo, J.; Chua, N. H., Chemical-inducible systems for regulated expression of plant genes. *Curr*
617 *Opin Biotechnol* **2000**, *11* (2), 146-51.
- 618 2. Keyes, W. M.; Mills, A. A., Inducible systems see the light. *Trends Biotechnol* **2003**, *21* (2), 53-5.
- 619 3. Mijakovic, I.; Petranovic, D.; Jensen, P. R., Tunable promoters in systems biology. *Curr Opin*
620 *Biotechnol* **2005**, *16* (3), 329-35.
- 621 4. de Boer, H. A.; Comstock, L. J.; Vasser, M., The tac promoter: a functional hybrid derived from
622 the trp and lac promoters. *Proc Natl Acad Sci U S A* **1983**, *80* (1), 21-5.
- 623 5. Lutz, R.; Bujard, H., Independent and tight regulation of transcriptional units in Escherichia coli
624 via the LacR/O, the TetR/O and AraC/I1-I2 regulatory elements. *Nucleic Acids Res* **1997**, *25* (6), 1203-10.
- 625 6. Urban, J. H.; Vogel, J., Translational control and target recognition by Escherichia coli small RNAs
626 in vivo. *Nucleic Acids Res* **2007**, *35* (3), 1018-37.
- 627 7. Cookson, N. A.; Mather, W. H.; Danino, T.; Mondragon-Palomino, O.; Williams, R. J.; Tsimring, L.
628 S.; Hasty, J., Queueing up for enzymatic processing: correlated signaling through coupled degradation.
629 *Mol Syst Biol* **2011**, *7*, 561.
- 630 8. Elowitz, M. B.; Leibler, S., A synthetic oscillatory network of transcriptional regulators. *Nature*
631 **2000**, *403* (6767), 335-8.
- 632 9. Gardner, T. S.; Cantor, C. R.; Collins, J. J., Construction of a genetic toggle switch in Escherichia
633 coli. *Nature* **2000**, *403* (6767), 339-42.
- 634 10. Becskei, A.; Serrano, L., Engineering stability in gene networks by autoregulation. *Nature* **2000**,
635 *405* (6786), 590-3.
- 636 11. Elowitz, M. B.; Levine, A. J.; Siggia, E. D.; Swain, P. S., Stochastic gene expression in a single cell.
637 *Science* **2002**, *297* (5584), 1183-6.
- 638 12. Ozbudak, E. M.; Thattai, M.; Kurtser, I.; Grossman, A. D.; van Oudenaarden, A., Regulation of
639 noise in the expression of a single gene. *Nat Genet* **2002**, *31* (1), 69-73.
- 640 13. Isaacs, F. J.; Dwyer, D. J.; Ding, C.; Pervouchine, D. D.; Cantor, C. R.; Collins, J. J., Engineered
641 riboregulators enable post-transcriptional control of gene expression. *Nat Biotechnol* **2004**, *22* (7), 841-
642 7.
- 643 14. Golding, I.; Cox, E. C., RNA dynamics in live Escherichia coli cells. *Proc Natl Acad Sci U S A* **2004**,
644 *101* (31), 11310-5.
- 645 15. Kalir, S.; Alon, U., Using a quantitative blueprint to reprogram the dynamics of the flagella gene
646 network. *Cell* **2004**, *117* (6), 713-20.
- 647 16. Golding, I.; Paulsson, J.; Zawilski, S. M.; Cox, E. C., Real-time kinetics of gene activity in individual
648 bacteria. *Cell* **2005**, *123* (6), 1025-36.
- 649 17. Balagadde, F. K.; Song, H.; Ozaki, J.; Collins, C. H.; Barnett, M.; Arnold, F. H.; Quake, S. R.; You, L.,
650 A synthetic Escherichia coli predator-prey ecosystem. *Mol Syst Biol* **2008**, *4*, 187.
- 651 18. Friedland, A. E.; Lu, T. K.; Wang, X.; Shi, D.; Church, G.; Collins, J. J., Synthetic gene networks that
652 count. *Science* **2009**, *324* (5931), 1199-202.
- 653 19. Juminaga, D.; Baidoo, E. E.; Redding-Johanson, A. M.; Batth, T. S.; Burd, H.; Mukhopadhyay, A.;
654 Petzold, C. J.; Keasling, J. D., Modular engineering of L-tyrosine production in Escherichia coli. *Appl*
655 *Environ Microbiol* **2012**, *78* (1), 89-98.
- 656 20. Daugherty, P. S.; Olsen, M. J.; Iverson, B. L.; Georgiou, G., Development of an optimized
657 expression system for the screening of antibody libraries displayed on the Escherichia coli surface.
658 *Protein Eng* **1999**, *12* (7), 613-21.
- 659 21. Caliendo, B. J.; Voigt, C. A., Targeted DNA degradation using a CRISPR device stably carried in the
660 host genome. *Nat Commun* **2015**, *6*, 6989.

- 661 22. Schnider-Keel, U.; Seematter, A.; Maurhofer, M.; Blumer, C.; Duffy, B.; Gigot-Bonnefoy, C.;
662 Reimann, C.; Notz, R.; Defago, G.; Haas, D.; Keel, C., Autoinduction of 2,4-diacetylphloroglucinol
663 biosynthesis in the biocontrol agent *Pseudomonas fluorescens* CHA0 and repression by the bacterial
664 metabolites salicylate and pyoluteorin. *J Bacteriol* **2000**, *182* (5), 1215-25.
- 665 23. Lee, S. K.; Chou, H. H.; Pflieger, B. F.; Newman, J. D.; Yoshikuni, Y.; Keasling, J. D., Directed
666 evolution of AraC for improved compatibility of arabinose- and lactose-inducible promoters. *Appl*
667 *Environ Microbiol* **2007**, *73* (18), 5711-5.
- 668 24. Grant, P. K.; Dalchau, N.; Brown, J. R.; Federici, F.; Rudge, T. J.; Yordanov, B.; Patange, O.;
669 Phillips, A.; Haseloff, J., Orthogonal intercellular signaling for programmed spatial behavior. *Mol Syst Biol*
670 **2016**, *12* (1), 849.
- 671 25. Scott, S. R.; Hasty, J., Quorum Sensing Communication Modules for Microbial Consortia. *ACS*
672 *Synth Biol* **2016**, *5* (9), 969-77.
- 673 26. Tashiro, Y.; Kimura, Y.; Furubayashi, M.; Tanaka, A.; Terakubo, K.; Saito, K.; Kawai-Noma, S.;
674 Umeno, D., Directed evolution of the autoinducer selectivity of *Vibrio fischeri* LuxR. *J Gen Appl Microbiol*
675 **2016**, *62* (5), 240-247.
- 676 27. Halleran, A.; Murray, R. M., Cell-free and in vivo characterization of Lux, Las, and Rpa quorum
677 activation systems in *E. coli*. *ACS Synth Biol* **2017**.
- 678 28. Gyorgy, A.; Jimenez, J. I.; Yazbek, J.; Huang, H. H.; Chung, H.; Weiss, R.; Del Vecchio, D., Isocost
679 Lines Describe the Cellular Economy of Genetic Circuits. *Biophys J* **2015**, *109* (3), 639-46.
- 680 29. Callura, J. M.; Cantor, C. R.; Collins, J. J., Genetic switchboard for synthetic biology applications.
681 *Proc Natl Acad Sci U S A* **2012**, *109* (15), 5850-5.
- 682 30. Carrier, T. A.; Keasling, J. D., Investigating autocatalytic gene expression systems through
683 mechanistic modeling. *J Theor Biol* **1999**, *201* (1), 25-36.
- 684 31. Bintu, L.; Buchler, N. E.; Garcia, H. G.; Gerland, U.; Hwa, T.; Kondev, J.; Phillips, R., Transcriptional
685 regulation by the numbers: models. *Curr Opin Genet Dev* **2005**, *15* (2), 116-24.
- 686 32. Salis, H.; Tamsir, A.; Voigt, C., Engineering bacterial signals and sensors. *Contrib Microbiol* **2009**,
687 *16*, 194-225.
- 688 33. Daber, R.; Sochor, M. A.; Lewis, M., Thermodynamic analysis of mutant lac repressors. *J Mol Biol*
689 **2011**, *409* (1), 76-87.
- 690 34. Gatti-Lafranconi, P.; Dijkman, W. P.; Devenish, S. R.; Hollfelder, F., A single mutation in the core
691 domain of the lac repressor reduces leakiness. *Microb Cell Fact* **2013**, *12*, 67.
- 692 35. Ike, K.; Arasawa, Y.; Koizumi, S.; Mihashi, S.; Kawai-Noma, S.; Saito, K.; Umeno, D., Evolutionary
693 Design of Choline-Inducible and -Repressible T7-Based Induction Systems. *ACS Synth Biol* **2015**, *4* (12),
694 1352-60.
- 695 36. Mannan, A. A.; Liu, D.; Zhang, F.; Oyarzun, D. A., Fundamental Design Principles for
696 Transcription-Factor-Based Metabolite Biosensors. *ACS Synth Biol* **2017**, *6* (10), 1851-1859.
- 697 37. Yokobayashi, Y.; Weiss, R.; Arnold, F. H., Directed evolution of a genetic circuit. *Proc Natl Acad*
698 *Sci U S A* **2002**, *99* (26), 16587-91.
- 699 38. Tang, S. Y.; Fazelinia, H.; Cirino, P. C., AraC regulatory protein mutants with altered effector
700 specificity. *J Am Chem Soc* **2008**, *130* (15), 5267-71.
- 701 39. Tang, S. Y.; Cirino, P. C., Design and application of a mevalonate-responsive regulatory protein.
702 *Angew Chem Int Ed Engl* **2011**, *50* (5), 1084-6.
- 703 40. Tashiro, Y.; Fukutomi, H.; Terakubo, K.; Saito, K.; Umeno, D., A nucleoside kinase as a dual
704 selector for genetic switches and circuits. *Nucleic Acids Res* **2011**, *39* (3), e12.
- 705 41. Tang, S. Y.; Qian, S.; Akinterinwa, O.; Frei, C. S.; Gredell, J. A.; Cirino, P. C., Screening for
706 enhanced triacetic acid lactone production by recombinant *Escherichia coli* expressing a designed
707 triacetic acid lactone reporter. *J Am Chem Soc* **2013**, *135* (27), 10099-103.

- 708 42. Taylor, N. D.; Garruss, A. S.; Moretti, R.; Chan, S.; Arbing, M. A.; Cascio, D.; Rogers, J. K.; Isaacs, F.
709 J.; Kosuri, S.; Baker, D.; Fields, S.; Church, G. M.; Raman, S., Engineering an allosteric transcription factor
710 to respond to new ligands. *Nat Methods* **2016**, *13* (2), 177-83.
- 711 43. Maranhao, A. C.; Ellington, A. D., Evolving Orthogonal Suppressor tRNAs To Incorporate
712 Modified Amino Acids. *ACS Synth Biol* **2017**, *6* (1), 108-119.
- 713 44. Xiu, Y.; Jang, S.; Jones, J. A.; Zill, N. A.; Linhardt, R. J.; Yuan, Q.; Jung, G. Y.; Koffas, M. A. G.,
714 Naringenin-responsive riboswitch-based fluorescent biosensor module for Escherichia coli co-cultures.
715 *Biotechnol Bioeng* **2017**, *114* (10), 2235-2244.
- 716 45. Daber, R.; Lewis, M., Towards evolving a better repressor. *Protein Eng Des Sel* **2009**, *22* (11),
717 673-83.
- 718 46. Kast, P., pKSS--a second-generation general purpose cloning vector for efficient positive
719 selection of recombinant clones. *Gene* **1994**, *138* (1-2), 109-14.
- 720 47. Thyer, R.; Filipovska, A.; Rackham, O., Engineered rRNA enhances the efficiency of
721 selenocysteine incorporation during translation. *J Am Chem Soc* **2013**, *135* (1), 2-5.
- 722 48. Takagi, M.; Nishioka, M.; Kakahara, H.; Kitabayashi, M.; Inoue, H.; Kawakami, B.; Oka, M.;
723 Imanaka, T., Characterization of DNA polymerase from Pyrococcus sp. strain KOD1 and its application to
724 PCR. *Appl Environ Microbiol* **1997**, *63* (11), 4504-10.
- 725 49. Gollihar, J. D., Jr. Methods in protein engineering and screening: from rational design to directed
726 evolution and beyond Ph.D. Dissertation, University of Texas, at Austin, 2015.
- 727 50. Ellefson, J. W.; Meyer, A. J.; Hughes, R. A.; Cannon, J. R.; Brodbelt, J. S.; Ellington, A. D., Directed
728 evolution of genetic parts and circuits by compartmentalized partnered replication. *Nature*
729 *Biotechnology* **2014**, *32* (1), 97-101.
- 730 51. Abil, Z.; Ellefson, J. W.; Gollihar, J. D.; Watkins, E.; Ellington, A. D., Compartmentalized partnered
731 replication for the directed evolution of genetic parts and circuits. *Nat Protoc* **2017**, *12* (12), 2493-2512.
- 732 52. Khlebnikov, A.; Datsenko, K. A.; Skaug, T.; Wanner, B. L.; Keasling, J. D., Homogeneous
733 expression of the P(BAD) promoter in Escherichia coli by constitutive expression of the low-affinity high-
734 capacity AraE transporter. *Microbiology* **2001**, *147* (Pt 12), 3241-7.
- 735 53. Rogers, J. K.; Guzman, C. D.; Taylor, N. D.; Raman, S.; Anderson, K.; Church, G. M., Synthetic
736 biosensors for precise gene control and real-time monitoring of metabolites. *Nucleic Acids Res* **2015**, *43*
737 (15), 7648-60.
- 738 54. Meyer, A. J.; Ellefson, J. W.; Ellington, A. D., Library generation by gene shuffling. *Current*
739 *protocols in molecular biology* **2014**, 15.12. 1-15.12. 7.
- 740 55. Salis, H. M.; Mirsky, E. A.; Voigt, C. A., Automated design of synthetic ribosome binding sites to
741 control protein expression. *Nat Biotechnol* **2009**, *27* (10), 946-50.
- 742 56. Lee, J. W.; Gyorgy, A.; Cameron, D. E.; Pyenson, N.; Choi, K. R.; Way, J. C.; Silver, P. A.; Del
743 Vecchio, D.; Collins, J. J., Creating Single-Copy Genetic Circuits. *Mol Cell* **2016**, *63* (2), 329-336.
- 744 57. Bassalo, M. C.; Garst, A. D.; Halweg-Edwards, A. L.; Grau, W. C.; Domaille, D. W.; Mutalik, V. K.;
745 Arkin, A. P.; Gill, R. T., Rapid and Efficient One-Step Metabolic Pathway Integration in E. coli. *ACS Synth*
746 *Biol* **2016**, *5* (7), 561-8.
- 747 58. West, S. C., Enzymes and molecular mechanisms of genetic recombination. *Annu Rev Biochem*
748 **1992**, *61*, 603-40.
- 749 59. Barrick, J. E.; Lenski, R. E., Genome dynamics during experimental evolution. *Nat Rev Genet*
750 **2013**, *14* (12), 827-39.
- 751 60. Alon, U.; Surette, M. G.; Barkai, N.; Leibler, S., Robustness in bacterial chemotaxis. *Nature* **1999**,
752 *397* (6715), 168-71.
- 753 61. Zhang, Y.; Lara-Tejero, M.; Bewersdorf, J.; Galan, J. E., Visualization and characterization of
754 individual type III protein secretion machines in live bacteria. *Proc Natl Acad Sci U S A* **2017**, *114* (23),
755 6098-6103.

- 756 62. Zelcbuch, L.; Antonovsky, N.; Bar-Even, A.; Levin-Karp, A.; Barenholz, U.; Dayagi, M.;
757 Liebermeister, W.; Flamholz, A.; Noor, E.; Amram, S.; Brandis, A.; Bareia, T.; Yofe, I.; Jubran, H.; Milo, R.,
758 Spanning high-dimensional expression space using ribosome-binding site combinatorics. *Nucleic Acids*
759 *Res* **2013**, *41* (9), e98.
- 760 63. Smanski, M. J.; Bhatia, S.; Zhao, D.; Park, Y.; L, B. A. W.; Giannoukos, G.; Ciulla, D.; Busby, M.;
761 Calderon, J.; Nicol, R.; Gordon, D. B.; Densmore, D.; Voigt, C. A., Functional optimization of gene clusters
762 by combinatorial design and assembly. *Nat Biotechnol* **2014**, *32* (12), 1241-9.
- 763 64. Larson, M. H.; Gilbert, L. A.; Wang, X.; Lim, W. A.; Weissman, J. S.; Qi, L. S., CRISPR interference
764 (CRISPRi) for sequence-specific control of gene expression. *Nat Protoc* **2013**, *8* (11), 2180-96.
- 765 65. Ghodasara, A.; Voigt, C. A., Balancing gene expression without library construction via a reusable
766 sRNA pool. *Nucleic Acids Res* **2017**, *45* (13), 8116-8127.
- 767 66. Gupta, A.; Reizman, I. M.; Reisch, C. R.; Prather, K. L., Dynamic regulation of metabolic flux in
768 engineered bacteria using a pathway-independent quorum-sensing circuit. *Nat Biotechnol* **2017**, *35* (3),
769 273-279.
- 770 67. Blattner, F. R.; Plunkett, G., 3rd; Bloch, C. A.; Perna, N. T.; Burland, V.; Riley, M.; Collado-Vides, J.;
771 Glasner, J. D.; Rode, C. K.; Mayhew, G. F.; Gregor, J.; Davis, N. W.; Kirkpatrick, H. A.; Goeden, M. A.; Rose,
772 D. J.; Mau, B.; Shao, Y., The complete genome sequence of Escherichia coli K-12. *Science* **1997**, *277*
773 (5331), 1453-62.
- 774 68. Kittleson, J. T.; Cheung, S.; Anderson, J. C., Rapid optimization of gene dosage in E. coli using
775 DIAL strains. *J Biol Eng* **2011**, *5*, 10.
- 776 69. Nielsen, A. A.; Der, B. S.; Shin, J.; Vaidyanathan, P.; Paralanov, V.; Strychalski, E. A.; Ross, D.;
777 Densmore, D.; Voigt, C. A., Genetic circuit design automation. *Science* **2016**, *352* (6281), aac7341.
- 778 70. Weber, E.; Engler, C.; Gruetzner, R.; Werner, S.; Marillonnet, S., A modular cloning system for
779 standardized assembly of multigene constructs. *PLoS One* **2011**, *6* (2), e16765.
- 780 71. Datsenko, K. A.; Wanner, B. L., One-step inactivation of chromosomal genes in Escherichia coli K-
781 12 using PCR products. *Proc Natl Acad Sci U S A* **2000**, *97* (12), 6640-5.
- 782 72. Thomason, L. C.; Costantino, N.; Court, D. L., E. coli genome manipulation by P1 transduction.
783 *Curr Protoc Mol Biol* **2007**, *Chapter 1*, Unit 1 17.
- 784 73. Reetz, M. T.; Carballeira, J. D., Iterative saturation mutagenesis (ISM) for rapid directed
785 evolution of functional enzymes. *Nat Protoc* **2007**, *2* (4), 891-903.

786

787

788

789

790

791

792

793

794